J. Phys. Chem. Solids
Conference Proceedings for the U.S. - Japan Seminar
Physics and Chemistry of C_{60} and Related Compounds

Fullerene Derivatives and Fullerene Superconductors

H. H. Wang, J. A. Schlueter, A. C. Cooper, J. L. Smart, M. E. Whitten, U. Geiser, K. D. Carlson, J. M. Williams, U. Welp, J. D. Dudek and M. A. Caleca

Chemistry and Materials Science Divisions
Argonne National Laboratory
9700 South Cass Avenue
Argonne, IL 60439

Abstract

A series of 1:1 C_{60} cycloaddition adducts, $C_{60}A$ (A = anthracene, butadiene, cyclopentadiene, and methylcyclopentadiene), has been synthesized. The products are cleanly separated and characterized by use of TGA, ^{1}H-NMR, IR, and mass spectrometry. Among these adducts, C_{60}(methylcyclopentadiene) showed the highest thermal stability and was doped with three equivalents of rubidium. The resulting Rb_3C_{60}(MeCp) is a semiconductor but can be thermally converted to the superconducting Rb_3C_{60} through a retro-Diels-Alder reaction. A one-step doping process to prepare Rb_3C_{60} crystals has been developed. The optimal doping condition occurs at ~300°C. High superconducting shielding fractions between 60 and 90% and sharp transition widths ($\Delta T_{10\text{-}90}$ between 4 and 0.7 K) were measured for these samples.

1. Introduction

C_{60}, a new allotrope of carbon, has attracted an intense amount of research interest[1]. In the past three years, C_{60} related materials have been shown to exhibit many interesting solid state properties, including ferromagnetism[2], photoconductivity[3], nonlinear optical behavior[4], and superconductivity[5]. Most of the superconducting compounds have the composition M_3C_{60}, where M is an alkali metal[6]. The superconducting transition temperatures (T_c's) range from 2 K to 33 K, depending on the cation size and the unit cell volume [5,7-12]. The spherical "superatom" C_{60} leads to a close-packed (*fcc*) cubic crystal structure in both C_{60} and M_3C_{60}[6]. Based on the cubic structures and the recent four-probe conductivity measurements, M_3C_{60} compounds are three-dimensional superconductors[13]. In the case of one-dimensional and two-dimensional organic superconductors, a highly ordered crystal structure is essential, and superconductivity is often hampered or suppressed by anion disorder, as observed in the $(TMTSF)_2ClO_4$ and β-$(BEDT\text{-}TTF)_2I_2Br$ salts[14]. Cation disorder in the M_3C_{60} compounds, however, seems to have a negligible effect on superconductivity. For example, $K_{1.5}Rb_{1.5}C_{60}$ with occupational disorder on the cation sites gave a T_c between the values of K_3C_{60} and Rb_3C_{60}[15], and $RbCs_2C_{60}$ with similar disorder was reported to give the highest T_c (33 K) among the known M_3C_{60} superconductors [10].

In addition to cation disorder, C_{60} atoms undergo a rapid librational rachet motion[16]. Although the rachet motion has been shown to slow down at low temperature, static merohedral disorder in C_{60} is still present [17]. We set out to prepare a series of C_{60} adducts, where an organic molecule is added onto the C_{60} moiety. With a "handle" attached to C_{60} moiety, the fast molecular rotation is expected to slow down in the solid state. In this article, we present four C_{60}

adducts, $C_{60}A$ (A = anthracene, cyclopentadiene, methylcyclopentadiene and butadiene) prepared via Diels-Alder reactions. The C_{60}(methylcyclopentadiene) compound showed the largest thermal stability among these compounds, and it was doped with three equivalents of rubidium. The physical properties of the resultant salt, Rb_3C_{60}(MeCp), were compared with that of the Rb_3C_{60}. Also presented in the article is a comparison among three different approaches for the synthesis of the superconducting Rb_3C_{60} salt.

2. Experimental

C_{60} was extracted from graphite soot (Strem Chemicals, Inc.) with toluene and separated on a Norit A/silica gel column with toluene as the eluant [18]. C_{60} crystals were prepared from C_{60} powders by use of sublimation procedures in the presence of a He carrier gas [19]. A typical yield of the crystals was around 70%, and the crystal sizes range from a few tenths of a millimeter to about 2 mm. Doping of the C_{60} crystals was carried out with three equivalents of rubidium in sealed quartz ampoules which were assembled in an argon-filled dry box.

Synthesis of C_{60} Adducts

Four 1:1 C_{60} adducts have been prepared, i.e., C_{60}(anthracene), C_{60}(cyclopentadiene), C_{60}(methylcyclopentadiene), and C_{60}(butadiene). The synthesis and separation of C_{60}(anthracene) has been described in the literature [20]. C_{60}(cyclopentadiene) [21], [C_{60}(Cp)], and C_{60}(methylcyclopentadiene), [C_{60}(MeCp)], were prepared at room temperature with C_{60} and freshly cracked Cp or MeCp dimers according to a literature procedure [22]. The separation was carried out on a silica gel column with hexane/methylene chloride as the eluant. The C_{60}(butadiene) was prepared by the reaction of C_{60} and butadiene sulfone in a quartz pressure tube in toluene at 100°C and 160 psi argon pressure. The product

was separated on a silica gel column with hexane/methylene chloride as the eluant for the first time, followed by carbon disulfide as the eluant for the second time.

ESR, AC Susceptibility and SQUID Measurements

ESR spectra were measured on an IBM ER-200 spectrometer (X-band, 9.4 GHz) with a TE_{102} rectangular cavity. AC susceptibility measurements were carried out on a Lake Shore 7221 AC susceptometer, and the SQUID measurements were performed on a Quantum Design magnetometer. During a SQUID measurement, T_c and transition width were determined by cooling the sample in zero field, then by applying a field of 1 G at 5 K and recording data while warming.

3. Results and Discussion

(A) C_{60} Derivatives from Cycloaddition

The C_{60} molecule was reported to undergo Diels-Alder cycloaddition [23]. The characterization of the C_{60} adducts based on cycloaddition, however, was hampered by the formation of multiply-substituted adducts as well as the facile retro-Diels-Alder reactions [24]. Recently, several cycloadditions to C_{60} have been reported that have been stabilized against retro-Diels-Alder reactions [25-27]. We found that by optimizing reaction conditions and C_{60}/diene ratios, the 1:1 adducts are the predominant species and can be isolated with use of column chromatography. Cyclopentadiene [21] and methylcyclopentadiene react with C_{60} at room temperature, but a higher reaction temperature (~100°C) is required for anthracene and 1,3-butadiene. Silica gel columns were used with either carbon disulfide or hexane/methylene chloride as eluants. The unreacted C_{60} was removed as the first fraction (purple band) from the column and was identified by

its IR and UV-VIS spectra. The second fraction (brown band) was the desired 1:1 adduct. Typical yield of the 1:1 adducts ranged from 10 to 30%. Higher adducts were clearly visible on the column, but are not characterized at present. IR, UV-VIS, Mass spectrometry, ^{1}H-NMR, and TGA (thermal gravimetric analysis) were used to characterize the adducts. The observations of the parent peak in mass spectra was usually difficult due to the facile retro-Diels-Alder reactions[25]. C_{60}, as well as the starting dienes, were usually observed in the laser-desorption mass spectra of a clearly separated adduct [20]. ^{1}H-NMR and TGA data were more informative and will be presented here.

The molecular structural models of the 1:1 C_{60} adducts constructed with MM2 force constants (Chem 3D-plus software, Cambridge Scientific Computing, Inc.) are shown in Figure 1 (a) - (d).

--- Figure 1 (a-d) here ---

As shown in Figure 1 (a), the planar anthracene molecule loses its aromaticity in the central six-membered ring and adds onto the C_{60} molecule through the anthracene 9- and 10-carbon positions. The ^{1}H-NMR spectrum of the C_{60}(anthracene) adduct is shown in Figure 2.

--- Figure 2 here ---

The A_2B_2 patterns centered around δ 7.83 and δ 7.52 ppm are due to the aromatic A and B protons (8 H's). The sharp singlet from the methine protons (X) at δ 5.89 ppm (2 H's) compares closely to that of the methine protons of $C_{60}H_2$ (δ 5.93 ppm)[28]. The results of the TGA of the 1:1 C_{60}(anthracene) adduct are shown in Figure 3.

--- Figure 3 here ---

The heating rate was 20°C/min with 5 °C resolution. The expected weight loss due to one equivalent of anthracene sublimation from a 1:1 C_{60}(anthracene) adduct is 19.84%. The observed weight loss was 19.97 %. Some decomposition was

observable at temperatures as low as ~110°C. The mid-point of the thermal decomposition as indicated by the maximum in the derivative plot was 194°C. The low decomposition onset is in agreement with the facile retro-Diels-Alder reactions. This suggests that adjusting the reaction temperature shifts the equilibrium position for the product distribution, with lower temperature favoring the adduct, as expected from entropy arguments.

The molecular model of C_{60}(butadiene) is shown in Figure 1 (b). The ^{1}H-NMR (in CS_2 with two drops of d_8-THF) of the C_{60}(butadiene) revealed a multiplet at δ 7.1 ppm (2 H's) which was assigned to the olefinic protons. The methylene protons appeared at δ 4.15 ppm (doublet, J= 4.1 Hz, 4 H's). Additional confirmation of this assignment comes from the ^{1}H-NMR (in CS_2 referenced to d_6-acetone) of C_{60}(1,1,4,4-d_4-butadiene) where all four methylene protons have been replaced by deuterons. The olefinic protons appeared as a sharp singlet at δ 7.1 ppm (2 H's), and the resonance absorption at 4.15 ppm disappeared. The symmetric nature of the ^{1}H-NMR spectrum suggested that the butadiene molecule is added to the C_{60} moiety through the 6-6 ring junction.

The C_{60}(cyclopentadiene) adduct has been reported in the literature [21]. Its molecular model is shown in Figure 1 (c). The ^{1}H-NMR ($CDCl_3$) indicated a singlet at δ 7.09 ppm (2 H's, olefinic), a singlet at δ 4.51 ppm (2 H's, methine), a doublet at δ 3.45 ppm (1 H, J ~ 9.9 Hz, methylene bridgehead), and another doublet at δ 2.52 ppm (1 H, J ~ 9.9 Hz, methylene bridgehead). All chemical shifts are consistent with the literature values [21], but we did not observe the small coupling (1.5 Hz) reported for the first two peaks. The NMR results are also consistent with the proposed molecular structure, i.e., the cyclopentadiene is added onto the C_{60} through the 6-6 ring junction. The stability of the C_{60}(cyclopentadiene) adduct is indicated by the TGA results in Figure 4.

--- Figure 4 here ---

The expected weight loss from a C_{60}(cyclopentadiene) adduct due to loss of cyclopentadiene is 8.40%. The observed total weight loss was 8.81%. The decomposition onset temperature was ~ 90°C, which is consistent with the reported decomposition at 95°C [21]. Also indicated in the weight loss derivative plot of TGA results in Figure 4 is the multiple-step decomposition process. Four local maxima, which indicate the decomposition mid-point temperatures, at ~100, 150, 210, and 275 °C were observed. The multiple maxima suggest that the cyclopentadiene moiety undergoes fragmentation and loses C_1 or C_2 units in a stepwise fashion but detailed mechanism awaits further studies.

The molecular model of C_{60}(methylcyclopentadiene) is shown in Figure 1 (d). The ^{1}H-NMR spectrum obtained in CS_2 containing two drops of CD_2Cl_2 is shown in Figure 5.

--- Figure 5 here ---

The spectrum consists of the following absorptions: a broad singlet at δ 6.68 ppm (1 H, olefinic), two singlets at δ 4.48 and 4.35 ppm, respectively (1 H each, methine protons), two doublets at δ 3.55 and 2.68 ppm, respectively (1 H each, J = 9.3 Hz, methylene bridgehead protons), and a singlet at δ 2.42 ppm (3 H's, methyl protons). The NMR spectrum supports the proposed molecular model and no other isomer was observed. TGA of the C_{60}(methylcyclopentadiene) adduct was also carried out. The expected weight loss from methylcyclopentadiene sublimation is 10.01%, and 10.60% was observed. The decomposition onset temperature was ~160°C. Two local maxima indicating the decomposition mid-points on the derivative plot were noted at 223 and 290°C, respectively. The multiple maxima indicate that the methylcyclopentadiene moiety also undergoes fragmentation during retro-Diels-Alder reaction, although at a higher temperature and in a different manner than the C_{60}(Cp) adduct.

The thermal stability of the four aforementioned C_{60} adducts is summarized in Table I. The decomposition onset and mid-point temperatures are both listed.

--- Table I here ---

Among the four C_{60} adducts, C_{60}(methylcyclopentadiene) gave the highest decomposition onset temperature. Due to its relatively high thermal stability, we carried out the alkali metal doping experiments described in the following section.

(B) Doping of C_{60}(methylcyclopentadiene)

In order to search for possible superconductivity in a C_{60} derivative salt, a doping experiment on C_{60}(methylcyclopentadiene), C_{60}(MeCp), was carried out. C_{60}(MeCp) were chosen because of its relative thermal stability. Powders of C_{60}(MeCp) were mixed with three equivalents of rubidium and heated to 150°C, or 10° below the decomposition onset temperature of C_{60}(MeCp), for two days. The resulting sample showed a clear ESR absorption. Results from line shape deconvolution analysis indicated two unresolved components in the sample. The broader line width component (28.5 G) consisted of 91% of the total integrated area and the narrower line width component (15.2 G) consisted of the remaining 9%. Temperature dependent ESR studies of the Rb doped C_{60}(MeCp) sample between 500 and 4 K are shown in Figure 6.

--- Figure 6 here ---

Between 350 and 100 K, both the overall peak-to-peak line width (ΔH) and the ESR spin susceptibility (χ) decrease with decreasing temperature. The decrease in χ with decreasing temperature between 350 and 100 K indicated a decrease in the carrier density and a semiconducting behavior [29]. At temperatures below 100 K, the line width leveled off at 1.5-2 G and the spin susceptibility showed a strong

rise. This behavior was Curie-Weiss and was caused by a minor paramagnetic component in the sample. A reasonable explanation is that the Curie tail arises from a minor component tentatively assigned as RbC_{60}(MeCp), and the major component is Rb_3C_{60}(MeCp), which behaves as a semiconductor.

Between 350 and 450 K, the line widths vary slightly from 27 G to 30 G and the relative spin susceptibilities scatter between 1.0 and 1.15. This behavior is reminiscent of the Pauli paramagnetism of a metallic sample. Above 450 K (177°C), which is higher than the C_{60}(MeCp) decomposition onset temperature, the spin susceptibility rises again. The increase in χ at high temperature is likely caused by the thermal decomposition of C_{60}(MeCp). We tested the sample for superconductivity after the high temperature ESR study and no sign of superconductivity was detected in an AC susceptibility measurement down to 5 K. For the high temperature ESR experiment, the sample had been heated above 200°C for an estimated two hours. In order to pursue the retro-Diels-Alder reaction in the presence of rubidium metal, the Rb_3C_{60}(MeCp) sample was heated at 250°C for 2 days. A clear superconducting signal (15% shielding fraction at 5 K) with an onset T_c at ~22K was observed. The same sample was heated at 250°C for five more days, and a stronger superconducting signal (21% shielding fraction at 5 K) was observed at a slightly higher onset temperature of 23 K. ESR analysis of the superconducting sample revealed three components: 15 G (4 %), 32 G (31 %), and 177 G (65 %). The compositions were calculated from the integrated area only and do not necessarily represent the molar concentration of each phases. In order to characterize this three-component mixture, a low temperature ESR study was performed. The results are listed in Table II.

-- Table II here --

As indicated in Table II, the broadest line (177 G) vanished quickly with decreasing temperature. The behavior was semiconducting and could not

account for the observed superconductivity. The 32 G phase became the predominant phase at low temperature, and was assignable to the well known superconducting Rb_3C_{60} phase. The assignment was reasonable because the sample could contain carbonaceous impurities from the decomposition of C_{60}(MeCp), resulting in line width broadening (32 G) similar to that reported for Rb_3C_{60} (22-32 G) from solution phase synthesis [30], which contained a small amount of solvent impurities. The remaining component (15 G phase) was ascribed to RbC_{60} or a small amount of undecomposed RbC_{60}(MeCp). The T_c of the thermally decomposed Rb_3C_{60}(MeCp) was 23 K and lower than the pure Rb_3C_{60} compound. The lowering of the T_c was likely caused by the impurities from decomposition as it was previously reported in the oxide superconductors [31].

At present, the doping experiment has been carried out only on C_{60}(MeCp). The semiconducting property of Rb_3C_{60}(MeCp) is likely caused by the inefficient packing due to the bulky MeCp function group. Future studies will explore the doping of other smaller C_{60} derivatives so that the rachet motion of the spherical C_{60} can be slowed while attempting to obtain the efficient packing of the *fcc* structure.

(C) A Comparison Between Solution Phase and Vapor Phase Synthesis of Rb_3C_{60}

The synthesis of M_3C_{60} superconducting thin film and bulk material is commonly done by use of the vapor phase doping procedure. A solution phase synthesis was originally carried out in toluene where C_{60} solution was allowed to react with molten alkali metals [9, 32]. An improved procedure by a change of solvent from dry toluene to toluene plus 10%(vol) benzonitrile was published recently [30]. The reaction scheme is shown as follows.

-- Scheme I here ---

In dry toluene, RbC_{60} precipitated upon the reduction of C_{60}. Further reduction of the solid RbC_{60} with molten rubidium was very slow. The isolated product was mostly RbC_{60} with a small amount of Rb_3C_{60} and the superconducting shielding fraction was below 7%. In toluene with 10% benzonitrile, the reduction of C_{60} became very efficient. The reaction scheme is outlined below.

-- Scheme II here --

Benzonitrile was reported as a redox catalyst in the literature [33, 34]. The PhCN molecule received one electron from the rubidium metal and formed the PhCN radical anion. The radical anion diffused through the bulk solution and transferred its unpaired electron to C_{60} even when the latter was far away from the metal surface to form C_{60} radical anion. The C_{60} radical anion was soluble in the polar solvent mixture and was further reduced to C_{60}^{3-} before it was precipitated out. This process greatly improved the electron transfer rate between C_{60} and alkali metal. Superconducting shielding fractions up to 50% (measured at 5 K without demagnetization) were observed after two hours of reaction time[30]. Variation of the amount of benzonitrile between 5 and 30% by volume did not change the product distribution. Large amounts of benzonitrile, however, resulted in the dissolution of Rb_3C_{60} and lowered the yield. Replacing benzonitrile with other organic solvents such as chlorobenzene or nitrobenzene, which had similar dielectric constants, simply failed to generate the superconducting material. This experiment further demonstrated the unique redox characteristics of benzonitrile.

The advantage of the solution phase synthesis is twofold. Firstly, the reaction is almost a homogeneous reaction and the intrinsic reaction rate is much faster than that of the solid state reaction. The typical reaction time is two hours, in sharp contrast to the days or weeks that are required by use of solid state doping. The short reaction time also makes scaling-up easy. Secondly, the

reaction temperature near 110°C, which is much lower than that required by the vapor phase method, makes possible the intercalation of the C_{60} derivatives which decompose at higher temperatures. The disadvantage of the solution phase synthesis at present is the trapping of trace amount of organic solvents, which lowers the quality of the samples.

Both solution [30] and vapor phase syntheses [15, 35] can yield samples with high superconducting shielding fractions. However, due to the fine particle sizes, the superconducting transition widths in these samples are quite broad. The 10-to-90% superconducting transition widths ($\Delta T_{10\text{-}90}$) are typically larger than 10 K. Sharp transition widths (< 1 K) have previously only been observed in resistivity measurements [13, 36]. We have developed a one-step process allowing the production of Rb_3C_{60} crystals which show sharp inductive superconducting transitions and high shielding fractions.

C_{60} crystals were prepared by sublimation in the presence of a He carrier gas. Typical crystal sizes range between a few tenths of a millimeter to ~2 mm. Approximately 10 to 30 mg of C_{60} crystals were accurately weighed and loaded into 3 mm or 4 mm quartz tubes. Three equivalents of rubidium metal were added to the tube in an argon filled dry box. These quartz tubes were then evacuated to 10^{-2} torr and flame sealed. The sealed tubes were heated in a furnace between 200 and 450°C.

The initial doping process was monitored with the use of an ESR spectrometer. The individual components can be estimated from the line shape deconvolution analysis. Two major components, RbC_{60} and Rb_3C_{60}, are always observed in these samples. The integrated ESR absorption of any specific phase is correlated to its molar concentration according to the following equations:

$$A_{RbC_{60}} = \chi_{RbC_{60}} \times [RbC_{60}]$$

and

$$A_{Rb_3C_{60}} = \chi_{Rb_3C_{60}} \times [Rb_3C_{60}]$$

where A is the integrated absorption, χ is the ESR spin susceptibility, and [RbC_{60}] is the molar concentration of RbC_{60}. The ratio $\chi_{Rb_3C_{60}}/\chi_{RbC_{60}}$ was previously established to be ~1.62 [37], which was used to calculate the molar ratio of Rb_3C_{60}/RbC_{60} in all samples.

Two samples were heated at 200 and 300°C, respectively, and monitored after brief quenching to room temperature by use of ESR approximately every 20 hours. The formation of the RbC_{60} and Rb_3C_{60} phases as a function of heating time is shown in Figure 7 (a, b).

--- Figure 7 (a, b) here ---

At 200°C, the growth rate for the RbC_{60} phase was much faster than that of the Rb_3C_{60} phase. The observation was consistent with the recent report that RbC_{60} is a stable line compound at temperatures above 433 K [38]. At 300°C, the initial growth rate of the RbC_{60} phase was still faster, but the growth rate of the Rb_3C_{60} phase was also significantly increased. The growth rates for both phases suggested a possible cross-over. However, for longer doping time (> 4 days) the ESR line widths became sharper for both phases. The 1:1 and 3:1 phases gave rise to 5.5 G and 8 G line widths, respectively. As the difference between the two line widths became smaller, and since the difference in g-values was always small, the line shape deconvolution analysis became unstable because of high correlations among the fitting parameters. No phase assignment could be made with the room temperature ESR data under those conditions.

Another sample was heated at 400°C. After 1 day, the sample gave a strong and narrow line width. The deconvolution analysis based on room temperature ESR data did not give a stable refinement due to the narrow line width and highly correlated refinement parameters. All samples were heated for a week before taking the SQUID measurements. The samples heated at 200, 300 and 400°C gave the following results (shielding fraction at 5 K, ΔT_{10-90}): (12%, 4.4 K), (23.5%,

3.0 K), and (65%, 1.8 K), respectively. The shielding fractions were correlated to the Rb_3C_{60} contents in the samples based on low temperature ESR analyses. The details are published elsewhere [37]. In general, doping of C_{60} crystals instead of powders with three equivalents of rubidium gave much sharper transition widths ($\Delta T_{10-90} \leq 4$ K). Higher doping temperatures gave rise to a higher superconducting shielding fraction and a sharper transition width. However, crystal exfoliation also increased with increasing doping temperature. Knowing the general trend, we carried out another doping experiment with the largest available C_{60} crystals. About 7~8 large C_{60} crystals (> 1 mm) were selected to be doped with three equivalents of Rb at 300°C. After 6 days of doping, some exfoliation on the crystal surface was still noticeable but most crystals remained intact. The sample quality was very good based on its sharp transition width ($\Delta T_{10-90} \sim 0.7$ K) and high shielding fraction (> 90%). The X-ray diffraction on these individual crystals gave relatively sharp diffraction maxima superimposed upon noticeable complete powder rings. These crystals of Rb_3C_{60} were not single but their quality was significantly better than that of compressed disks. A brief comparison of the solution and vapor phase syntheses is summarized in Table III.

-- Table III here ---

4. Conclusion

Significant progress on the C_{60} related chemistry has been made over the past few years. In contrast to early speculations, the C_{60} molecule is actually quite reactive toward small molecules such as oxygen, halogens, borane, amines, azides, dienes,...etc. [39]. The chemical and physical properties of these novel C_{60} derivatives will remain interesting to explore in the years to come.

In addition to new C_{60} superconductors with even higher T_c's, there is a need to develop a procedure for growing single crystals of M_3C_{60} for fundamental studies. Direct vapor phase doping generates high quality samples but the crystals are not single. Solution phase techniques such as recrystallization or electrocrystallization may offer a viable route to single crystals in the future.

Acknowledgment

Work at Argonne National Laboratory is sponsored by the US Department of Energy (DOE), Office of Basic Energy Sciences, Division of Materials Sciences, under Contract W-31-109-ENG-38. A.C.C., J.L.S., M.E.W., J.D.D., and M.A.C. are undergraduate student research participants sponsored by the Argonne Division of Educational Programs from Alma College, Alma, MI; Western Montana College, Dillon, MT; Clemson University, Clemson, SC; University of Wisconsin-Platteville, Platteville, WI, and Wagner College, Staten Island, NY, respectively.

References

1. Krätschmer, W.; Lamb, L. D.; Fostiropoulos, K.; Huffman, D. R. *Nature* **1990**, *347*, 354.
2. Allemand, P.-M.; Khemani, K. C.; Koch, A.; Wudl, F.; Holczer, K.; Donovan, S.; Grüner, G.; Thompson, J. D. *Science (Washington, D.C.)* **1991**, *253*, 301.
3. Wang, Y. *Nature* **1992**, *356*, 585.
4. Flom, S. R.; Pong, R. G. S.; Bartoli, F. J.; Kafafi, Z. H. *Phys. Rev. B Rapid Commun.* **1992**, *46*, 15598.
5. Hebard, A. F.; Rosseinsky, M. J.; Haddon, R. C.; Murphy, D. W.; Glarum, S. H.; Palstra, T. T. M.; Ramirez, A. P.; Kortan, A. R. *Nature* **1991**, *350*, 600.
6. Stephens, P. W.; Mihaly, L.; Lee, P. L.; Whetten, R. L.; Huang, S.-M.; Kaner, R.; Diederich, F.; Holczer, K. *Nature* **1991**, *351*, 632.
7. Rosseinsky, M. J.; Ramirez, A. P.; Glarum, S. H.; Murphy, D. W.; Haddon, R. C.; Hebard, A. F.; Palstra, T. T. M.; Kortan, A. R.; Zahurak, S. M.; Makhija, A. V. *Phys. Rev. Lett.* **1991**, *66*, 2830.
8. Holczer, K.; Klein, O.; Huang, S.-M.; Kaner, R. B.; Fu, K.-J.; Whetten, R. L.; Diederich, F. *Science (Washington, D.C.)* **1991**, *252*, 1154.
9. Wang, H. H.; Kini, A. M.; Savall, B. M.; Carlson, K. D.; Williams, J. M.; Lathrop, M. W.; Lykke, K. R.; Parker, D. H.; Wurz, P.; Pellin, M. J.; Gruen, D. M.; Welp, U.; Kwok, W.-K.; Fleshler, S.; Crabtree, G. W.; Schirber, J. E.; Overmyer, D. L. *Inorg. Chem.* **1991**, *30*, 2962.
10. Tanigaki, K.; Ebbesen, T. W.; Saito, S.; Mizuki, J.; Tsai, J. S.; Kubo, Y.; Kuroshima, S. *Nature* **1991**, *352*, 222.
11. Tanigaki, K.; Hirosawa, I.; Ebbesen, T. W.; Mizuki, J.; Shimakawa, Y.; Kubo, Y.; Tsai, J. S.; Kuroshima, S. *Nature* **1992**, *356*, 419.

12. Rosseinsky, M. J.; Murphy, D. W.; Fleming, R. M.; Tycko, R.; Ramirez, A. P.; Siegrist, T.; Dabbagh, G.; Barrett, S. E. *Nature* **1992**, *356*, 416.

13. Xiang, X.-D.; Hou, J. G.; Crespi, V. H.; Zettl, A.; Cohen, M. L. *Nature* **1993**, *361*, 54.

14. Williams, J. M.; Ferraro, J. R.; Thorn, R. J.; Carlson, K. D.; Geiser, U.; Wang, H. H.; Kini, A. M.; Whangbo, M.-H. *Organic Superconductors (Including Fullerenes): Synthesis, Structure, Properties and Theory*; Prentice Hall: New Jersey, 1992; .

15. Chen, C.; Kelty, S. P.; Lieber, C. M. *Science* **1991**, *253*, 886.

16. Johnson, R. D.; Yannoni, C. S.; Dorn, H. C.; Salem, J. R.; Bethune, D. S. *Science* **1992**, *255*, 1235.

17. Barrett, S. E.; Tycko, R. *Phys. Rev. Lett.* **1992**, *69*, 3754.

18. Scrivens, W. A.; Bedworth, P. V.; Tour, J. M. *J. Am. Chem. Soc.* **1992**, *114*, 7917.

19. Liu, J. Z.; Dykes, J. W.; Lan, M. D.; Klavins, P.; Shelton, R. N.; Olmstead, M. M. *Appl. Phys. Lett.* **1993**, *62(5)*, 531.

20. Schlueter, J. A.; Seaman, J. M.; Taha, S.; Cohen, H.; Lykke, K. R.; Wang, H. H.; Williams, J. M. *J. Chem. Soc., Chem. Commun.* **1993**, 972.

21. Rotello, V. M.; Howard, J. B.; Yadav, T.; Conn, M. M.; Viani, E.; Giovane, L. M.; Lafleur, A. L. *Tetrahedron Letters* **1993**, *34*, 1561.

22. Darkwa, J.; Giolando, D. M.; Murphy, C. J.; Rauchfuss, T. B. *Inorg. Synth.* **1990**, *27*, 51.

23. Wudl, F. *Acc. Chem. Res.* **1992**, *25*, 157.

24. Wudl, F.; Hirsch, A.; Khemani, K. C.; Suzuki, T.; Allemand, P.; Koch, A.; Eckert, H.; Srdanov, G.; Webb, H. M. *ACS Symposium Series* **1992**, *481*, 161.

25. Rubin, Y.; Khan, S.; Freedberg, D. I.; Yeretzian, C. *J. Am. Chem. Soc.* **1993**, *115*, 344.

26. Prato, M.; Suzuki, T.; Foroudian, H.; Li, Q.; Khemani, K.; Wudl, F.; Leonetti, J.; Little, R. D.; White, T.; Rickborn, B.; Yamogo, S.; Nakamura, E. *J. Am. Chem. Soc.* **1993**, *115*, 1594.

27. Hoke, S. H., II; Molstad, J.; Dilettato, D.; Jay, M. J.; Carson, D.; Kahr, B.; Cooks, R. G. *J. Org. Chem.* **1992**, *57*, 5069.

28. Henderson, C. C.; Cahill, P. A. *Science* **1993**, *259*, 1885.

29. Also suggested by Dr. K. Holczer during the conference that a thermally activated singlet and triplet hopping process can give rise to the broad transition between 100 and 350 K. Detailed measurements await further study.

30. Schlueter, J. A.; Wang, H. H.; Lathrop, M. W.; Geiser, U.; Carlson, K. D.; Dudek, J. D.; Yaconi, G. A.; Williams, J. M. *Chem. Mater.* **1993**, *5*, 720.

31. Wang, H. H.; Kini, A. M.; Kao, H.-C. I.; Appelman, E. H.; Thompson, A. R.; Botto, R. E.; Carlson, K. D.; Williams, J. M.; Chen, M. Y.; Schlueter, J. A.; Gates, B. D.; Hallenbeck, S. L.; Despotes, A. M. *Inorg. Chem.* **1988**, *27*, 5.

32. Wang, H. H.; Kini, A. M.; Savall, B. M.; Carlson, K. D.; Williams, J. M.; Lykke, K. R.; Wurz, P.; Parker, D. H.; Pellin, M. J.; Gruen, D. M.; Welp, U.; Kwok, W.-K.; Fleshler, S.; Crabtree, G. W. *Inorg. Chem.* **1991**, *30*, 2838.

33. Austin, E.; Alonso, R. A.; Rossi, R. A. *J. Org. Chem.* **1991**, *56*, 4486.

34. Swartz, J. E.; Stenzel, T. T. *J. Am. Chem. Soc.* **1984**, *106*, 2520.

35. McCauley, J. P., Jr.; Zhu, Q.; Coustel, N.; Zhou, O.; Vaughan, G. B. M.; Idziak, S. H. J.; Fischer, J. E.; Tozer, S. W.; Groski, D. M.; Bykovetz, N.; Lin, C. L.; McGhie, A. R.; Allen, B. H.; Romanow, W. J.; Demenstein, A. M.; Smith, A. B., III *J. Am. Chem. Soc.* **1991**, *113*, 8537.

36. Ogata, H.; Inabe, T.; Hoshi, H.; Maruyama, Y.; Achiba, Y.; Suzuki, S.; Kikuchi, K.; Ikemoto, I. *Jpn. J. Appl. Phys.* **1992**, *31*, L166.

37. Schlueter, J. A.; Welp, U.; Wang, H. H.; Geiser, U.; Williams, J. M.; Bauer, M. J.; Cho, J. M.; Smart, J. L.; Taha, S. A. *Physica C* , submitted.

38. Zhu, Q.; Zhou, O.; Fischer, J. E.; McGhie, A. R.; Romanow, W. J.; Strongin, R. M.; Cichy, M. A.; Smith, A. B., III *Phys. Rev. B., Rapid Commun.* **1993**, *47*, 13948.

39. Taylor R.; Walton, D. R. M. *Nature* **1993**, *363*, 685.

Figure Captions

Figure 1 Idealized molecular structural models constructed with MM2 energy minimization for C_{60}(A) adducts, A = anthracene (a), butadiene, (b) cyclopentadiene (c), and methylcyclopentadiene (d).

Figure 2 ^{1}H-NMR spectrum of the 1:1 C_{60}(anthracene) adduct in CD_2Cl_2.

Figure 3 Thermal gravimetric analysis (TGA) results on C_{60}(anthracene) showing the weight loss with increasing temperature and the derivative of the weight loss.

Figure 4 TGA results on C_{60}(cyclopentadiene) adduct showing the weight loss and the multiple local maxima in the derivative weight loss plot.

Figure 5 ^{1}H-NMR spectrum of the C_{60}(methylcyclopentadiene) adduct in CS_2 referenced to CD_2Cl_2.

Figure 6 Variable temperature ESR studies of Rb_3C_{60}(MeCp) with liquid He cryostat for temperatures below 200 K and N_2 temperature controller for temperatures above 200 K, showing the temperature dependence of the peak-to-peak line widths (triangles) and the relative spin susceptibilities (squares).

Figure 7 The formation of RbC_{60} and Rb_3C_{60} phases during the doping of C_{60} crystals with three equivalents of rubidium at 200 (a) and 300°C (b).

Table I. The decomposition onset and midpoint temperatures of C_{60} adducts based on TGA analyses

Adduct	Onset (°C)	Midpoint (°C)
C60(Cp)	90	150
C60(butadiene)	100	168
C60(An)	110	194
C60(MeCp)	160	223

Table II Low temperature ESR results of the thermally decomposed Rb_3C_{60}(MeCp) indicating three components

Temperature K	RbC60(MeCp) or RbC60	Rb3C60	Other phase	R[a]
296	14.8 G (4 %)	32.3 G (31 %)	177 G (65 %)	2.1 %
200	5.1 G (15 %)	8 G (45 %)	29 G (40 %)	2.9 %
100	2.3 G (45 %)	5.4 G (55 %)	–	7.5 %
60	1.8 G (44 %)	3.0 G (56 %)	–	8.4 %

[a]*Refinement agreement factor of fit:* $R = 100\%(\Sigma\ |obs - calc|/\Sigma\ |obs|)$.

About 450 data points were used in each spectrum.

Table III A summary of the synthesis of Rb_3C_{60}

Procedure	Reaction Time	Reaction Temperature	T_c (K)	Shielding Fraction[a]	ΔT_{10-90} (K)
Solution synthesis (powders)	2-4 hours (fast)	~110°C	28.6	50%	> 14 K
Vapor synthesis (powders)	2 days to 2 weeks (slow)	200-450 °C	29-29.6	~100%	> 10 K
Vapor synthesis (crystals)	> 1 week (slow)	200-450 °C	30.5	~90%	4 – 0.7 K

[a]Highest observed shielding fraction measured at 5 K without demagnetization.

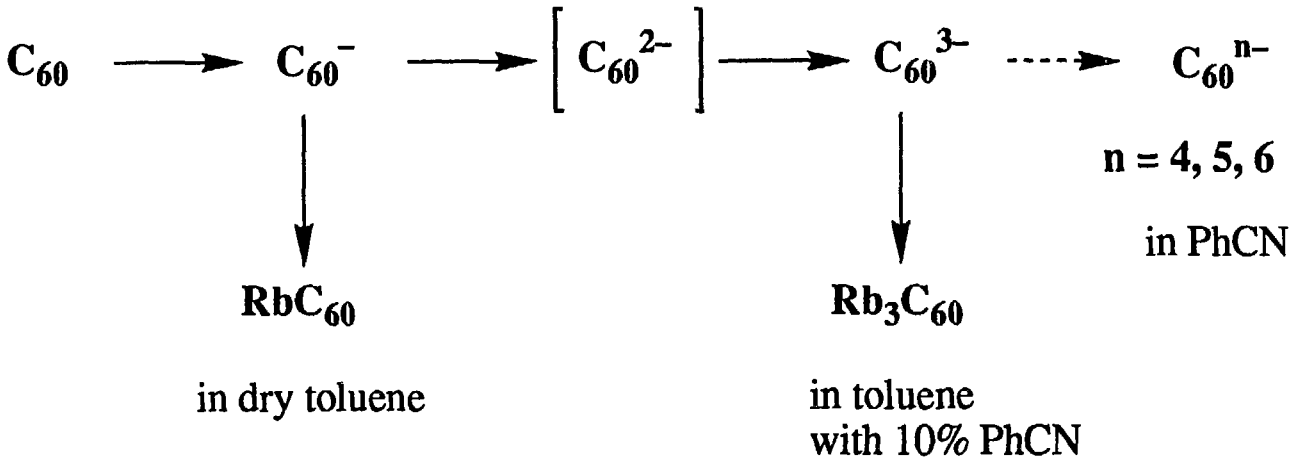

Scheme I Solution phase synthesis of Rb_3C_{60}

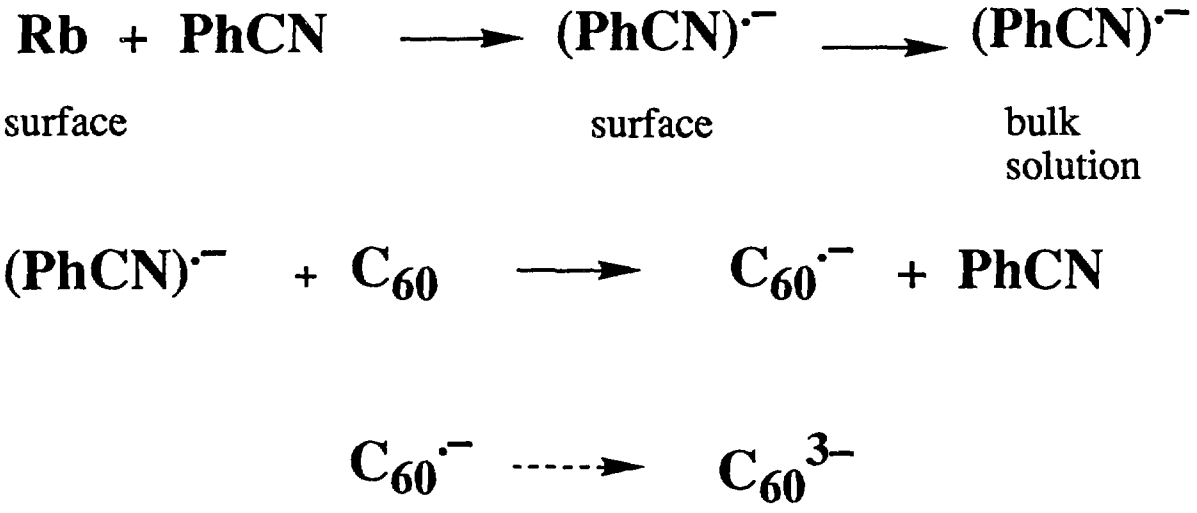

Scheme II Benzonitrile served as a redox catalyst

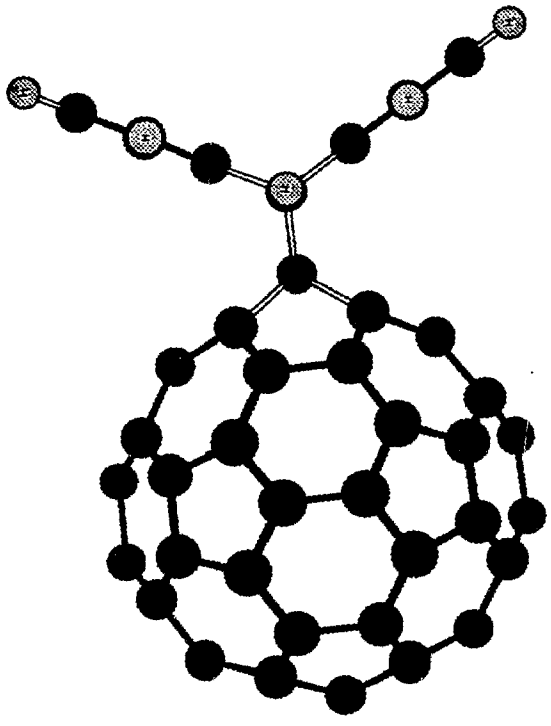

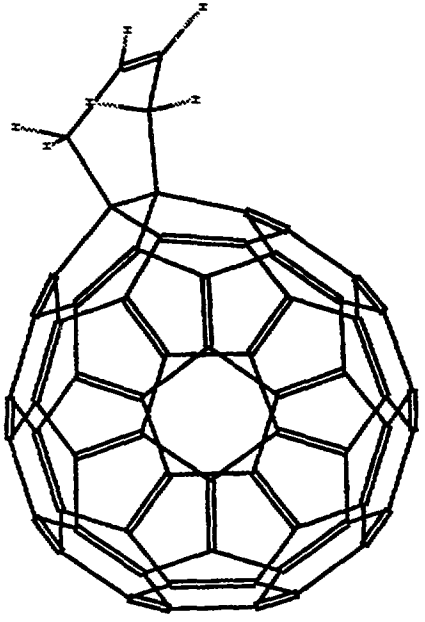

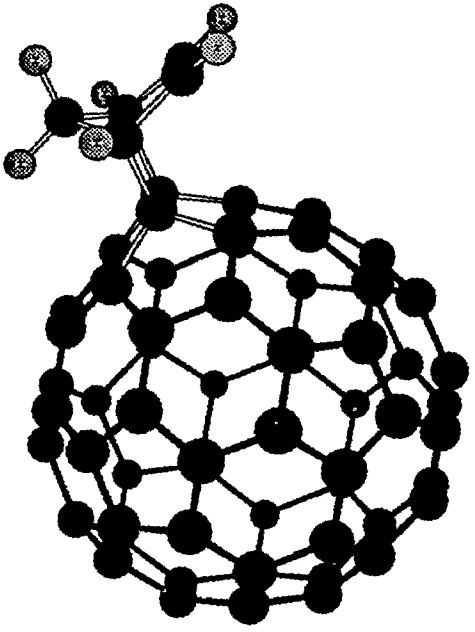

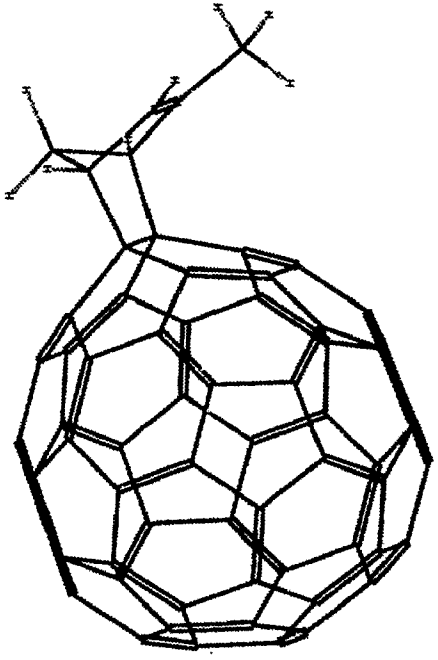

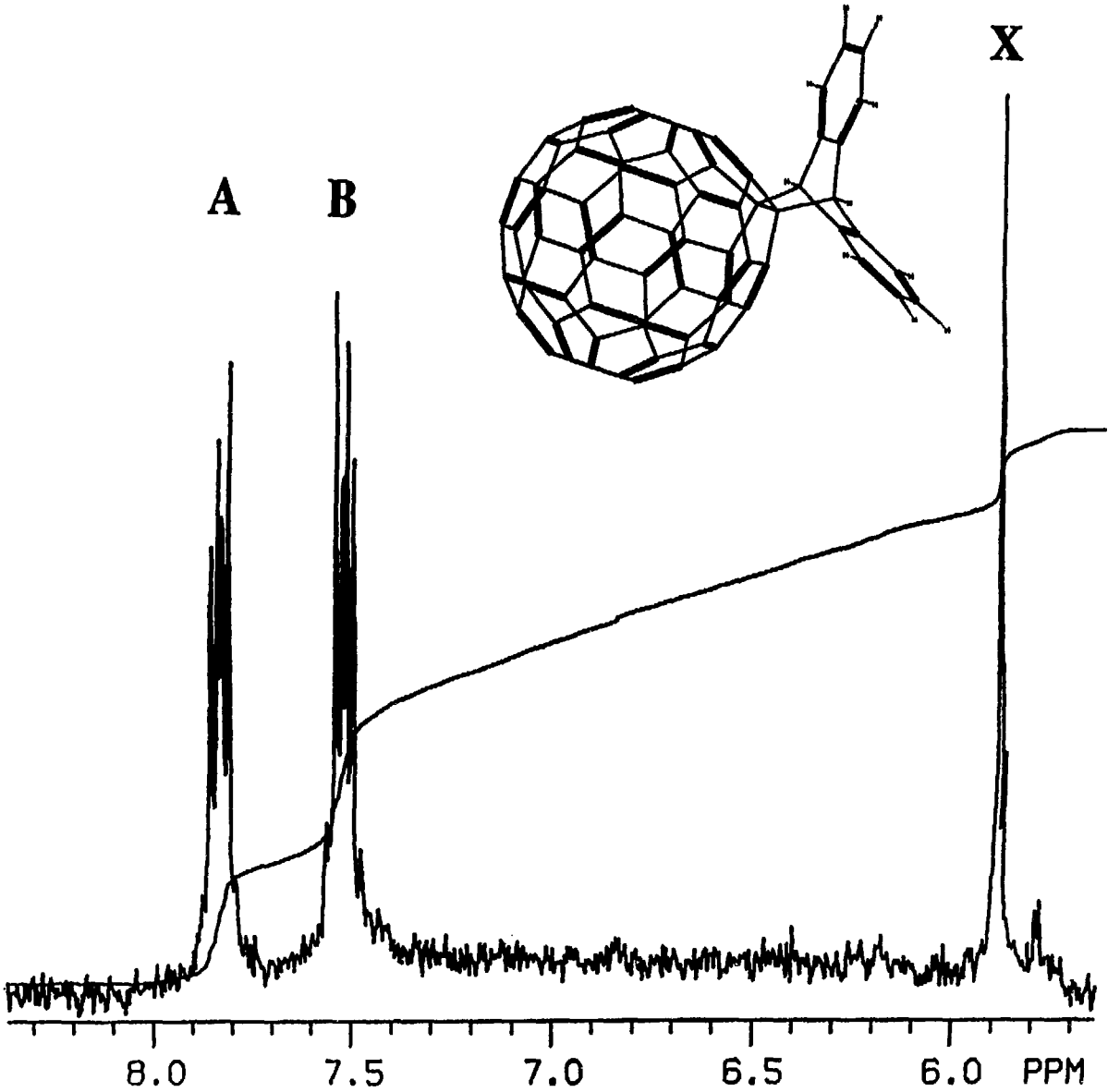
A
B
X
8.0
7.5
7.0
6.5
6.0
PPM

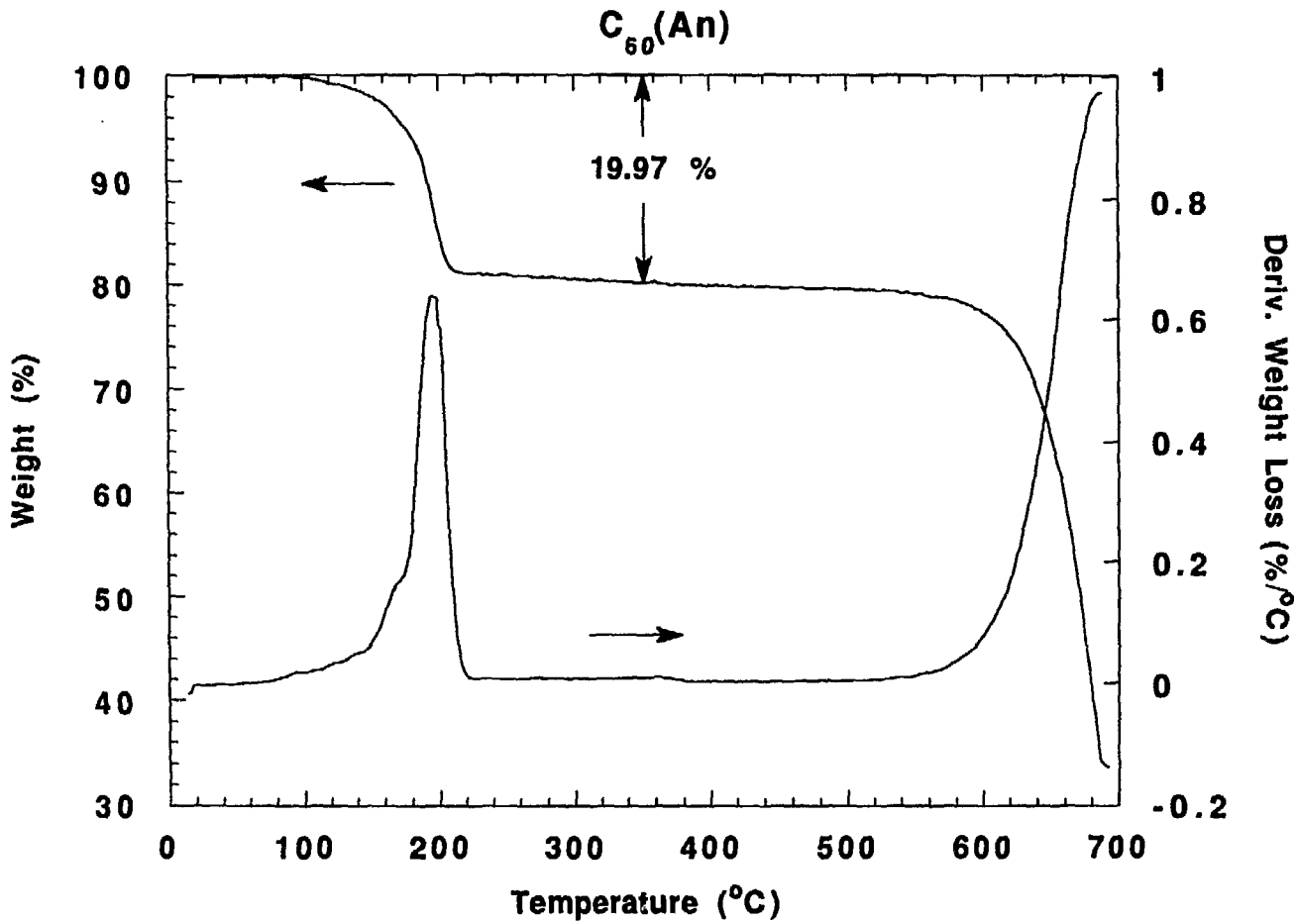
C60(An)
19.97 %
Weight (%)
Deriv. Weight Loss (%/°C)
Temperature (°C)
100
90
80
70
60
50
40
30
1
0.8
0.6
0.4
0.2
0
-0.2
0
100
200
300
400
500
600
700

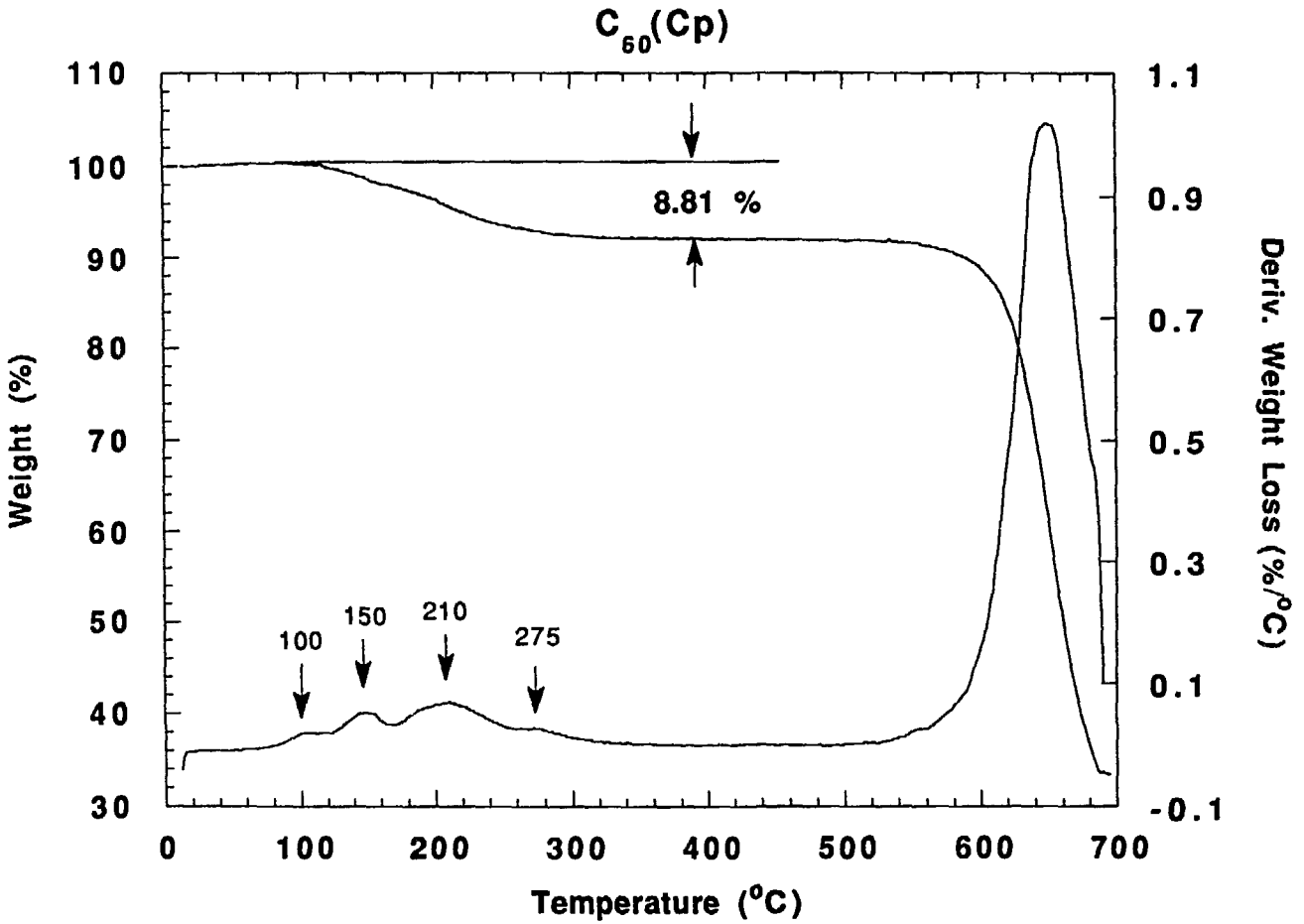
C60(Cp)
8.81 %
100
150
210
275
Weight (%)
Deriv. Weight Loss (%/°C)
Temperature (°C)
110
100
90
80
70
60
50
40
30
1.1
0.9
0.7
0.5
0.3
0.1
-0.1
0
100
200
300
400
500
600
700

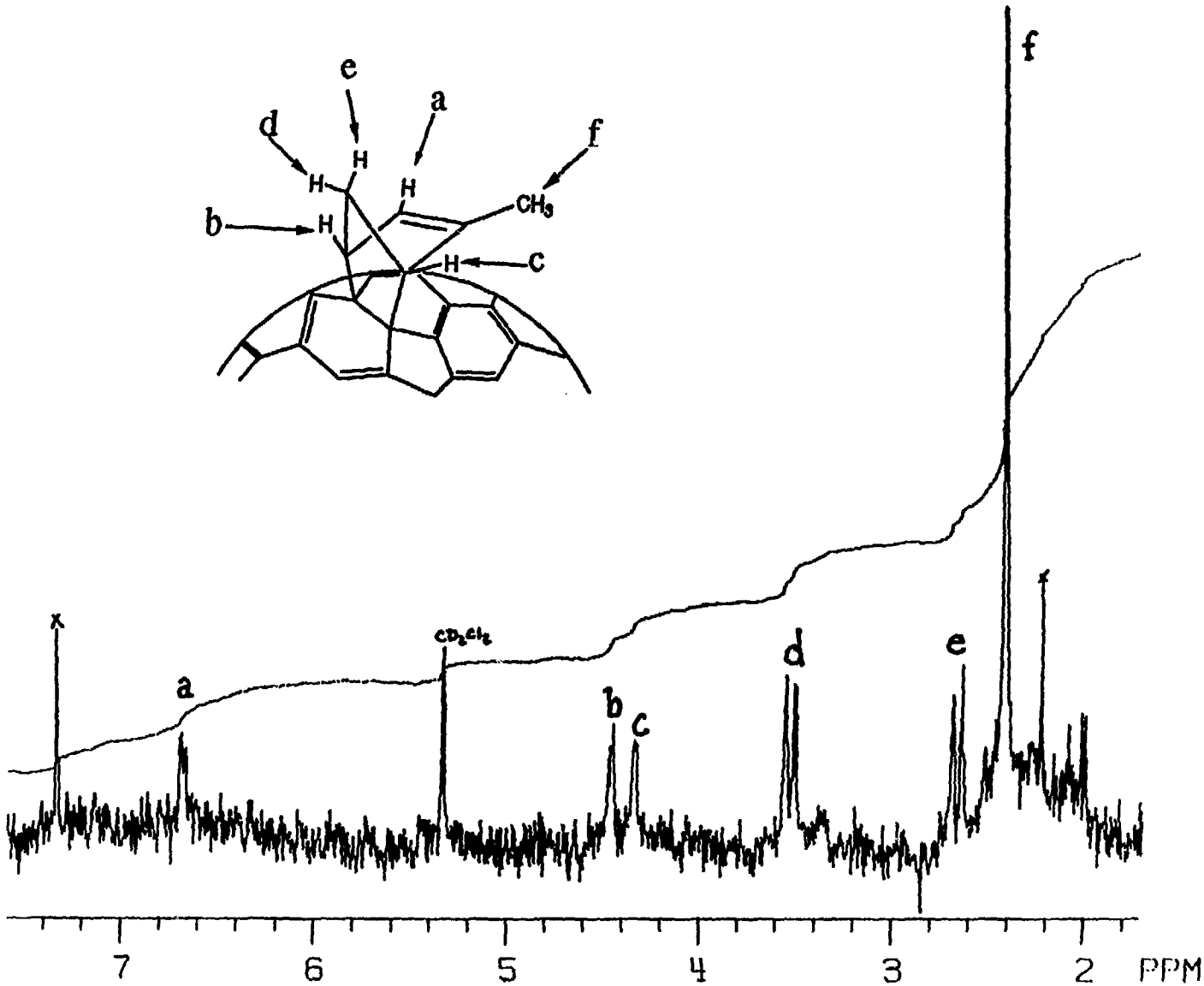
e
a
d
f
H
H
H
CH3
b
H
H
C
f
X
a
CD2Cl2
b
c
d
e
f
7
6
5
4
3
2
PPM

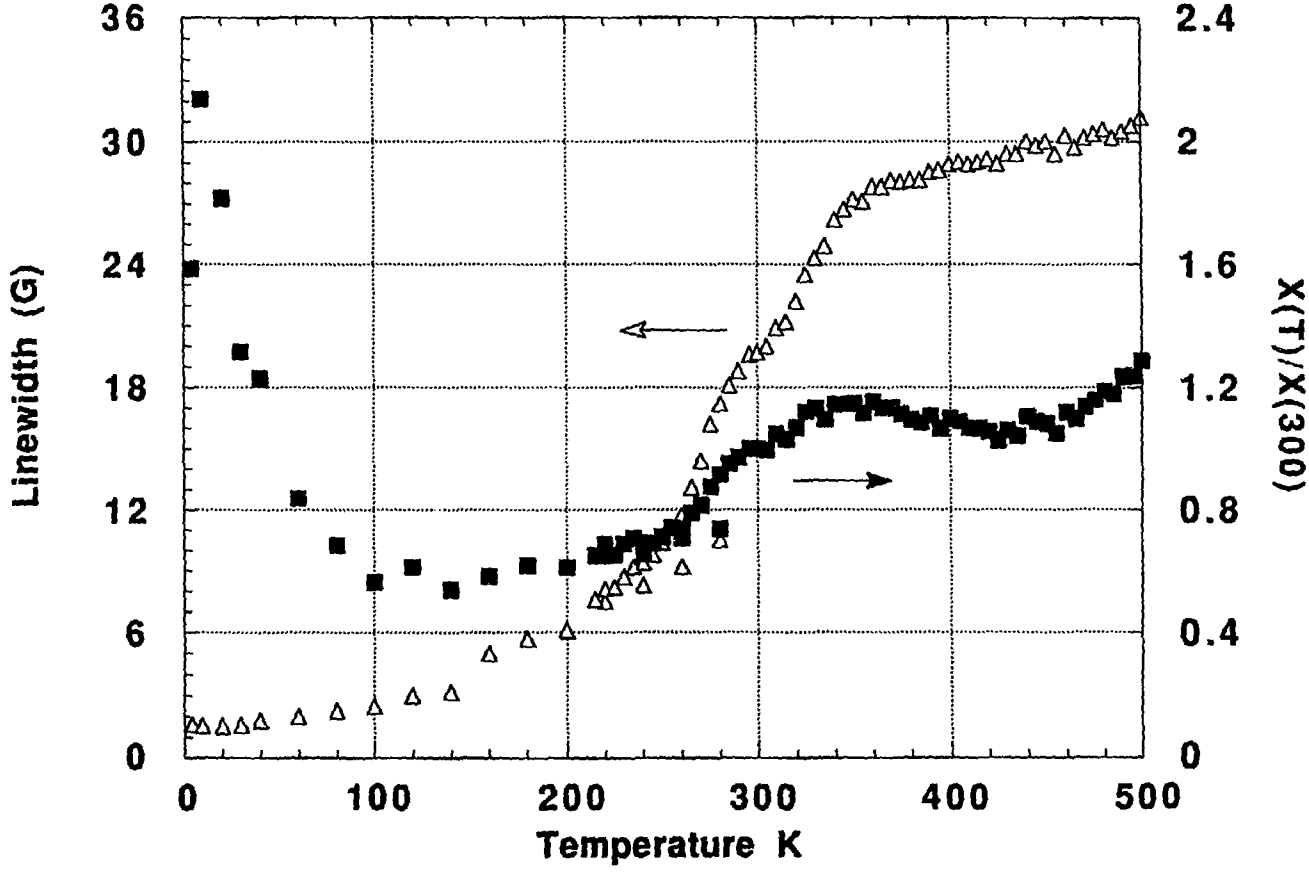
Linewidth (G)
X(T)/X(300)
Temperature K
36
30
24
18
12
6
0
2.4
2
1.6
1.2
0.8
0.4
0
0
100
200
300
400
500

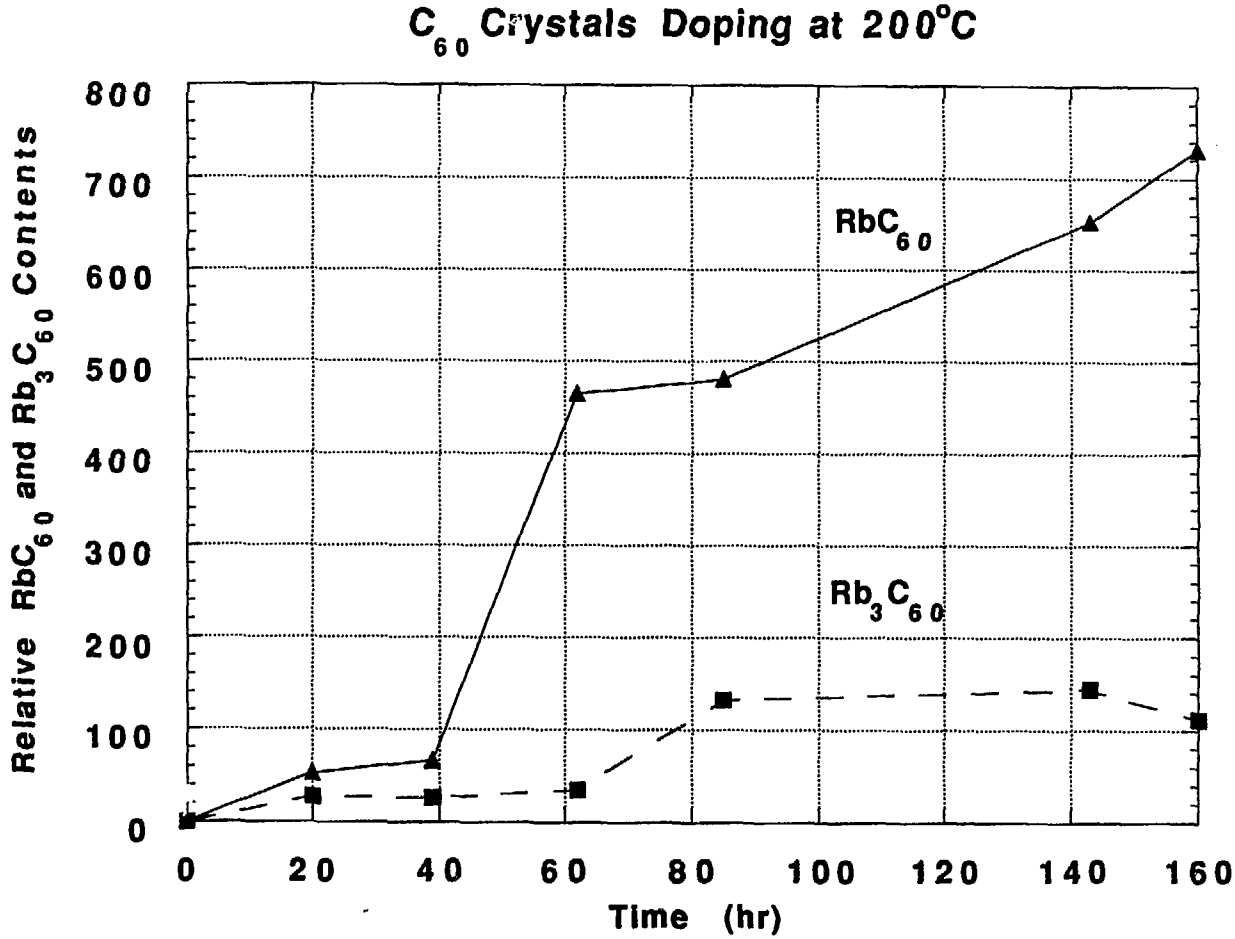
C_{60} Crystals Doping at 200°C
Relative RbC_{60} and Rb_3C_{60} Contents
800
700
600
500
400
300
200
100
0
0
20
40
60
80
100
120
140
160
Time (hr)
RbC_{60}
Rb_3C_{60}

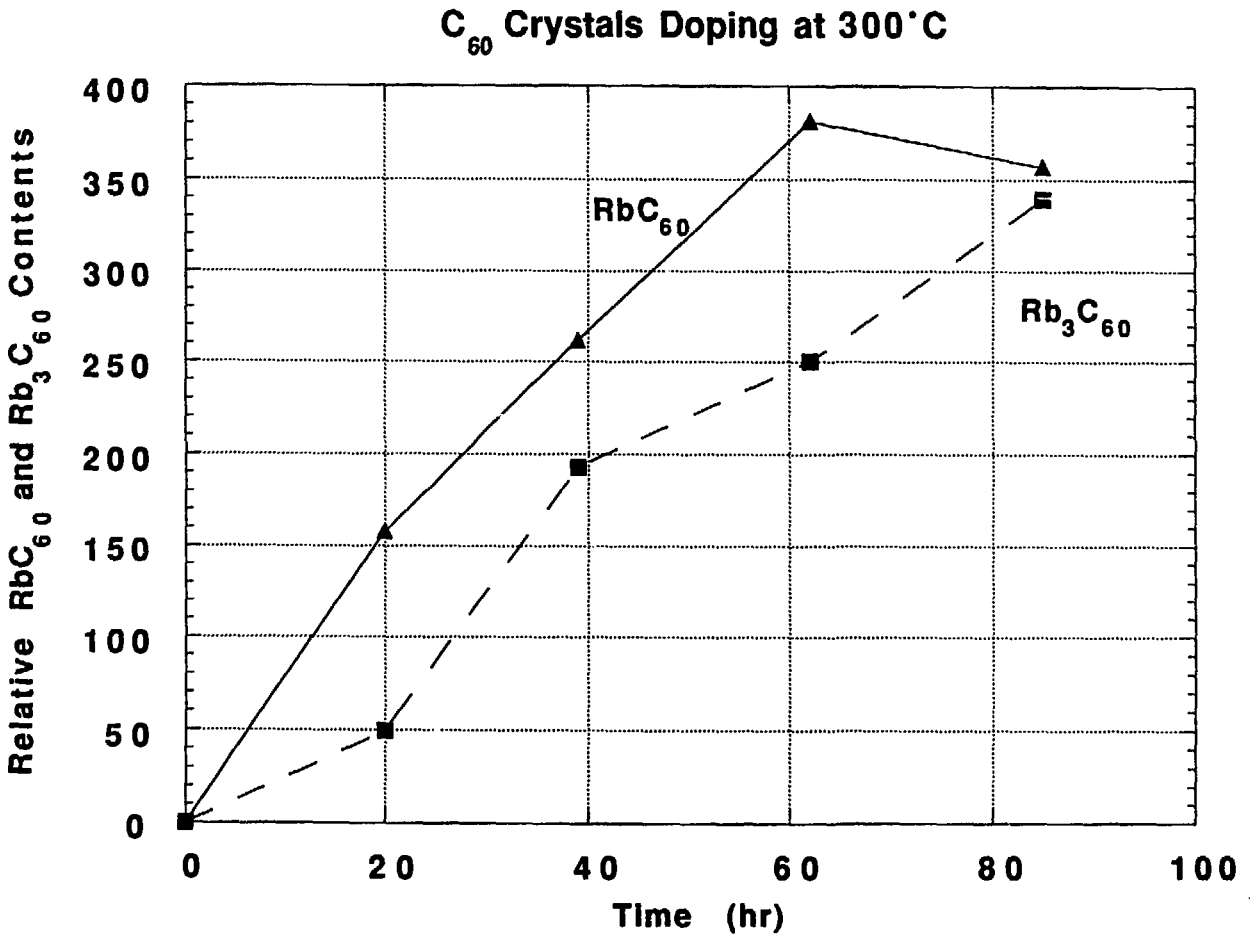
C60 Crystals Doping at 300°C
Relative RbC60 and Rb3C60 Contents
400
350
300
250
200
150
100
50
0
0
20
40
60
80
100
Time (hr)
RbC60
Rb3C60